ELSEVIER

Journal of Organometallic Chemistry 538 (1997) 63–74

Journal of Organometallic Chemistry

Synthesis, crystal structures and some properties of dimethylsilylene-bridged ansa-permethyltitanocene [Ti(IV), (III) and (II)] complexes

Vojtech Varga [a], Jörg Hiller [b], Róbert Gyepes [c], Miroslav Polášek [a], Petr Sedmera [d], Ulf Thewalt [b], Karel Mach [a,*]

[a] *J. Heyrovský Institute of Physical Chemistry, Academy of Sciences of the Czech Republic, Dolejškova 3, 182 23 Prague 8, Czech Republic*
[b] *Sektion für Röntgen- und Elektronenbeugung, Universität Ulm, D-89069 Ulm, Germany*
[c] *Department of Inorganic Chemistry, Charles University, Hlavova 2030, 128 40 Prague 2, Czech Republic*
[d] *Institute of Microbiology, Academy of Sciences of the Czech Republic, 142 20 Prague 4, Czech Republic*

Received 22 August 1996; revised 25 October 1996

Abstract

Dimethylsilylene-bridged complexes $Me_2Si(C_5Me_4)_2TiCl$ (**2**), $Me_2Si(C_5Me_4)_2Ti[\eta^2\text{-}C_2(SiMe_3)_2]$ (**3**) and $Me_2Si(C_5H_4)_2Ti[\eta^2\text{-}C_2(SiMe_3)_2]$ (**4**) have been prepared by the general methods which are known for obtaining of analogous non-bridged titanocene complexes. X-ray crystal structures of $Me_2Si(C_5Me_4)_2TiCl_2$ (**1**), **2**, and **3** reveal that the dihedral angle ϕ between the least-squares planes of cyclopentadienyl rings increases in the order **2** < **3** < **1**.

Comparison with the structures of analogous $(C_5HMe_4)_2Ti$ and $(C_5Me_5)_2Ti$ compounds shows that the value of ϕ increases in the series $(C_5Me_5)_2Ti < (C_5HMe_4)_2Ti < Me_2Si(C_5Me_4)_2Ti$, e.g. in the bis(trimethylsilyl)acetylene complexes from 41.1° for $(C_5Me_5)_2Ti[\eta^2\text{-}C_2(SiMe_3)_2]$ (**9**) to 50.0° for $(C_5HMe_4)_2Ti[\eta^2\text{-}C_2(SiMe_3)_2]$ (**8**) and to 53.5° for **3**. Compounds **3**, **8** and **9** induce the head-to-tail dimerization of 1-hexyne with the selectivity of 72%, 21% and ca. 100% respectively. The discrepancy between the selectivities and the values of ϕ for **3** and **8** is accounted for by a larger flexibility of the titanocene skeleton in **8**, affording a larger space for a non-specific coordination of 1-hexyne. The effects of the μ-Me_2Si group in **2** and **3** on some of their properties are compared with the effects of Me and H substituents in the non-ansa compounds with controversial results. For instance, the affinity of **2** to 2-methyltetrahydrofuran approaches that of $(C_5H_2Me_3)_2TiCl$ whereas the shift of the $\nu(C{\equiv}C)$ vibration in **3** indicates a stronger metal–acetylene bond than in **9**.

Keywords: Ansa-permethyltitanocene; Titanium; L-hexyne; Dimethylsilylene-bridged; Crystal structures; Dimerization

1. Introduction

The Lewis acidity of early transition metals in metallocene complexes is smoothly controlled by Me substituents at the cyclopentadienyl ligands [1,2]. In the titanocene series, the electron donation effect of Me groups strongly lowers the energy gap between HOMO and LUMO as indicated by UPS [3] and by other spectral data [4,5] and decreases the electrochemical oxidation potential of titanocene dichlorides [6]. The absence of steric hindrance in methylated cyclopentadienyltitanium trichlorides $(C_5H_{5-n}Me_n)TiCl_3$ ($n = 0$, 1, 3–5) allowed us to establish incrementally decreasing rates of the reduction by Et_2AlCl with an increasing number of Me groups [7]. Similar investigations on electronic effects of the trimethylsilyl group $SiMe_3$ have so far afforded ambiguous results, denoting the $SiMe_3$ group as an electron acceptor with respect to hydrogen [8,9] or an electron donor stronger than the Me group [10,11]. Recently, the dependency of the investigated property on its nature has been emphasized [12].

The influence of a bridging μ-$SiMe_2$ group, widely used to synthesize ansa-metallocene dichlorides as precursors in soluble Brintzinger–Kaminsky catalysts for stereospecific polymerizations of α-olefins [13], has been evaluated in terms of steric effects [14] whereas the electronic effect has not been considered. Neglect of the latter seemed to be justified by electrochemical

* Corresponding author.

PII S0022-328X(96)06917-3

measurements showing that reduction potentials of the $Me_2Si(C_5H_4)_2MCl_2$ (M = Ti, Zr) compounds are only slightly lower than those of the metallocene dichlorides [15]. In ferrocenophanes, the bridging μ-$SiMe_2$ group does not change the half-wave oxidation potential of $Fe(\eta^5\text{-}C_5H_4)_2SiMe_2$ against ferrocene whilst the methyl-substituted ferrocenophanes exert a decrease with the increment of 50 mV per one Me group [16], practically the same as in the series of methylated ferrocenes [3]. Accordingly, the chemical reduction of $Me_2Si(C_5H_4)_2TiCl_2$ proceeds smoothly in the presence of coordinating ligands and some derivatives of Ti(III) [17,18] and Ti(II) [19] are known. A considerable reluctance of μ-$(CH_2)_2(C_5H_4)_2TiCl_2$ to yield Ti(II) products or products of their rearrangement has been accounted for by the structural rigidity of the ansa-titanocene species which makes the activation of the cyclopentadienyl C–H bonds to be more difficult [20]. On the other hand, a smooth formation of the $(C_5H_{5-n}Me_n)_2Ti[\eta^2\text{-}C_2(SiMe_3)_2]$ (n = 0–5) complexes and the thermal generation of titanocene species thereof followed by their rearrangement have recently been demonstrated [21]. The permethylated complex $(C_5Me_5)_2Ti[\eta^2\text{-}C_2(SiMe_3)_2]$ appeared to be the superior catalyst of linear head-to-tail dimerization of terminal acetylenes whereas other members of this series were inactive in this reaction except the complex for $n = 4$ which showed a negligible activity and a low selectivity. This sharp change in the catalytic behaviour suggests a strong steric control of the catalytic species by the size of coordination space at the open side of the titanocene skeleton [22].

In this work we report the syntheses of the μ-$SiMe_2$ bridged monochloride $Me_2Si(C_5Me_4)_2TiCl$ (**2**) and bis(trimethylsilyl)acetylene complexes $Me_2Si(C_5Me_4)_2Ti[\eta^2\text{-}C_2(SiMe_3)_2]$ (**3**) and $Me_2Si(C_5H_4)_2Ti[\eta^2\text{-}C_2(SiMe_3)_2]$ (**4**), the crystal structures of $Me_2Si(C_5Me_4)_2TiCl_2$ (**1**), **2** and **3**, some spectroscopic properties of **2**, **3** and **4**, and the catalytic behaviour of **3** towards 1-hexyne. The emphasis is laid on the comparison of steric and electronic effects with those of highly methyl-substituted titanocene derivatives.

2. Experimental details

The synthesis of $Me_2Si(C_5Me_4)_2TiCl_2$ (**1**) and $Me_2Si(C_5H_4)_2TiCl_2$ (**5**) were carried out under argon and the compounds were then handled in air. Their reductions and subsequent manipulations, and most of the spectroscopic measurements were carried out under vacuum using all-sealed glass devices equipped with breakable seals.

2.1. Methods

^1H and ^{13}C NMR spectra were measured on a Varian VXR-400 spectrometer (400 MHz and 100 MHz respectively) in C_6D_6 at 25 °C. Chemical shifts (given in the δ scale) were referenced to the solvent signal (δ_H 7.15 ppm, δ_C 128.0 ppm). EPR spectra were recorded on an ERS-220 spectrometer (Centre for Production of Scientific Instruments, German Academy of Sciences, Berlin, Germany) in the X-band. A variable-temperature unit STT-3 was used for the measurement in the range −140 to +23 °C. UV–vis spectra were measured in the range 270–2000 nm on a Varian Cary 17D spectrometer using all-sealed quartz cuvettes (Hellma). Mass spectra were measured on a Jeol D-100 spectrometer at 70 eV (mass peaks of intensity not below 5% and important peaks are only reported). Samples in capillaries were opened and inserted into the direct inlet under argon. Infrared spectra were obtained on a UR-75 (Zeiss, Jena, Germany) or on a Mattson Galaxy 2020 spectrometer. Hexane or toluene solutions were filled into KBr cuvettes under argon. KBr pellets of solid samples were prepared in a glovebox (Labmaster 130, mBraun) under purified nitrogen and were measured in a gas-proof cuvette. GC analyses of volatile products of thermolysis of **3** were performed on a Chrom 5 gas chromatograph (Laboratory Instruments, Prague, Czech Republic) using 10% SE-30 on a Chromaton N-AW-DMCS column. Analogous GC-MS analyses were carried out on a Hewlett Packard gas chromatograph (5890 series II) equipped with a mass spectrometric detector (5971 A) and a capillary column SPB-1 (Supelco).

2.2. Chemicals

The solvents tetrahydrofuran (THF), 2-methyltetrahydrofuran (MTHF), hexane, toluene, and benzene-d_6 were purified by conventional methods, dried by refluxing over $LiAlH_4$ and stored as solutions of dimeric titanocene $(C_{10}H_8)[(C_5H_5)Ti(\mu\text{-}H)]_2$ [23]. Bis(trimethylsilyl)acetylene (BTMSA) (Fluka) was degassed, stored as a solution of dimeric titanocene for 4 h and distilled in vacuum into ampoules. Magnesium turnings (purum for Grignard reactions) were obtained from Fluka. Me_2SiCl_2 (Aldrich) was handled by the syringe technique under argon. Tetramethylcyclopentadiene was prepared from tetramethylcyclopentenone in two steps: the reduction with $LiAlH_4$ gave the alcohol and this was dehydrated by adding a catalytic amount of iodine [24]. BuLi in hexane (1.6 M) (Chemetall, Frankfurt a.M.) was handled by the syringe technique under argon. $Me_2Si(C_5H_4)_2TiCl_2$ (**5**) was prepared following the published procedure [15] and was characterized by MS, IR and ^1H and ^{13}C NMR spectra. The MS spectra differed from the published data [25] by higher intensi-

ties of the fragment ions compared to $M^{+\cdot}$; this is due to a longer residence time of ions in the ionization chamber.

2.3. Preparation of $Me_2Si(C_5HMe_4)_2$

The procedure described by Jutzi and Dickbreder [26] was followed, starting from 17.5 g (143 mmol) of $C_5H_2Me_4$. At variance, the reaction between lithium tetramethylcyclopentadienide and Me_2SiCl_2 in THF was completed only after 4 h of reflux. The yellow oily product was according to GC analysis a single compound and was not further purified by crystallization. Yield 9.0 g (42%). IR spectrum of a thin film agreed with literature data for $Me_2Si(C_5HMe_4)_2$ obtained in Nujol [27]. EI-MS (direct inlet, 70 eV, 50–70 °C; m/z(%)): 300(M^+, 8), 298(2), 253(2.5), 179(100), 163(3.5), 137(4), 133(3), 122(5.5), 121(7.5), 120(5), 119(11), 107(3.5), 105(8), 91(5), 75(4.5), 73(30), 59(25). Elemental analysis: 300.2268, error $+0.5 \times 10^{-3}$ for $C_{20}H_{32}Si$.

2.4. Preparation of $Me_2Si(C_5Me_4)_2TiCl_2$ (1)

$Me_2Si(C_5HMe_4)_2$ (4 g, 13.3 mmol) was diluted in 400 ml of THF and BuLi in hexane (1.6 M, 16.6 ml) was added. After stirring for 1 h this solution was added to a slurry obtained by adding BuLi in hexane (1.6 M, 8.3 ml) to 1.46 ml of $TiCl_4$ (13.3 mmol) in 100 ml of THF. The mixture was refluxed under argon for 2 days. The solution was reduced to ca. 200 ml and then 200 ml of aqueous HCl was added at room temperature. The crystalline material which separated from the mixture was filtered, washed with methanol and crystallized from a chloroform–methanol mixture. The pure compound was crystallized from toluene. Yield of brown-red crystals of $Me_2Si(C_5Me_4)_2TiCl_2$ was 2.0 g (36%).

MS (direct inlet, 70 eV, 170–180 °C; m/z(%)): 416(M^+, 32), 401(3), 381(64), 380(92), 365(100), 345(28), 343(16), 329(20), 321(17), 282(13), 243(7), 177(46), 59(25). IR (KBr)(cm^{-1}): 2938(m,sh), 2905(s), 2866(m,sh), 1498(m), 1450(m), 1406(m), 1376(s), 1357(s), 1329(s), 1269(s), 1260(s), 1150(m), 1131(m), 1017(s), 842(s), 829(m,sh), 812(s), 776(s), 763(m), 680(s), 652(m), 624(w), 618(w), 476(s). ^1H NMR ($CDCl_3$): δ 1.011 (s, 6H, $SiMe_2$), 1.825 (s, 12 H, Me), 2.097 (s, 12 H, Me). ^{13}C NMR ($CDCl_3$): δ 3.13 (q, 2C), 13.68 (q, 4C), 16.10 (q, 4C), 92.92 (s, 2C), 129.76 (s, 4C), 143.39 (s, 4C). The MS and NMR spectra are in agreement with published data [26].

2.5. Preparation of $Me_2Si(C_5Me_4)_2TiCl$ (2)

$Me_2Si(C_5Me_4)_2TiCl_2$ 0.2 g (0.5 mmol) was largely dissolved in toluene (15 ml) and butyllithium (0.1 M in hexane, 5 ml) was added under stirring. The mixture was stirred and heated to 60 °C for 1 h. A small part of the solid $Me_2Si(C_5Me_4)_2TiCl_2$ remained unreacted. The solution was separated and the solvents were evaporated in vacuum. The brown residue was repeatedly extracted with hexane. The volume of the extracted solution was reduced to 5 ml and the saturated solution was poured away. The residue was crystallized from hot hexane to give 0.14 g (74%) of brown crystals. The crystals were used for the X-ray data collection and the preparation of solutions in toluene and MTHF for spectroscopic measurements.

MS (direct inlet, 70 eV, 140–150 °C; m/z(%)): 381(M^+, 100), 366(7), 365(11), 346(31), 345(82), 343(45), 341(21), 339(9), 330(15), 257(6), 243(7), 190.5(M^{2+}, 2), 177(6), 172.5(6), 165(10), 59(11). IR (KBr)(cm^{-1}): 2918(vs), 2859(s), 1454(w), 1379(m), 1306(w), 1254(s), 1130(w), 1017(m), 843(s), 814(vs), 770(s), 675(vs), 475(vs). UV–vis (λ_{max}, toluene): 350 > 410(sh) ~ 445(sh) > 525 > 600(sh) nm (in MTHF, the same bands were found). EPR spectra in toluene and MTHF solutions in the range 23 to −140 °C are summarized in Table 1. All the results give evidence that compound **2** is monomeric both in the gas phase and in the toluene and MTHF solutions.

2.6. Preparation of $Me_2Si(C_5Me_4)_2Ti[\eta^2\text{-}C_2(SiMe_3)_2]$ (3)

$Me_2Si(C_5Me_4)_2TiCl_2$ 0.8 g (2.0 mmol) and Mg turnings (0.243 g, 10 mmol) were charged into an ampoule equipped with a Teflon-coated magnetic stirrer. The ampoule was evacuated and BTMSA (0.5 ml, 2.2 mmol) and THF (30 ml) were distilled-in on a vacuum line. The mixture was frozen by liquid nitrogen, sealed off

Table 1
ESR parameters of $Me_2Si(C_5Me_4)_2TiCl$ (**2**) and $(C_5H_{5-n}Me_n)_2TiCl$ (n = 3–5) in toluene and in MTHF solutions and frozen glasses [a]

Compound	Solvent	g_{iso}	a_{Ti} (G)	g_z	g_x	g_y	g_{av}	Ref.
2	Toluene	1.9725	—	2.000	1.988	1.929	1.972	This work
n = 3	Toluene	1.965	—	2.001	1.986	1.915	1.967	[1]
n = 4	Toluene	1.964	—	2.000	1.985	1.910	1.965	[1]
n = 5	Toluene	1.957	—	1.999	1.984	1.889	1.956	[1]
2	MTHF	1.9726 [b]	—					
		1.9826 [c]	10.0	1.999	1.985	1.966	1.983	This work
n = 3	MTHF	1.965 [b]	—					[1]
		1.979 [c]	12.0	2.001	1.983	1.954	1.979	

[a] The isotropic spectra were measured at 23 °C; the anisotropic spectra were measured at −130 °C for toluene solutions and at −140 °C for MTHF solutions. The accuracy of the g_{iso}-value determination using an Mn^{2+} standard ($M_I = -1/2$ line at g = 1.9860) was ±0.0003. The assignment of g-tensor components is taken from Ref. [28].
[b] The species uncoordinated by MTHF.
[c] The species coordinated by MTHF.

and stirred at room temperature for 2 days. Finally, it was heated to 60 °C for 6 h. The pale orange-brown solution was poured away from unreacted magnesium and was evaporated in vacuum. The brown residue was extracted with 50 ml of hexane in a closed system until the orange colour of the fresh extract ceased. A solid product partly precipitated from the orange solution. The volume of the solution was reduced to ca. 10 ml and after standing overnight the solution was poured away from the solid. The latter was dried in vacuum and dissolved in hot toluene. Bright orange crystals were obtained by slow cooling of the above solution to room temperature. These crystals were used for the X-ray data collection and the spectroscopic and chemical investigations. They were low-soluble in hexane and moderately soluble in toluene. Yield of crystalline **3** was 0.4 g (39%).

^{1}H NMR (C_6D_6): δ −0.054 (s, 18H, $SiMe_3$), 0.302 (s, 6H, $SiMe_2$), 1.177 (s, 12H, Me), 2.631 (s, 12H, Me). ^{13}C NMR (C_6D_6): δ 3.07 (q, 2C, $SiMe_2$), 4.20 (q, 6C, $SiMe_3$), 14.36 (q, 4C), 14.86 (q, 4C), 103.74 (s, 2C), 132.88 (s, 4C), 139.78 (s, 4C), 254.86 (s, 2C). IR (KBr)(cm^{-1}): 2953(s), 2901(s), 1622(m,sh), 1580(m), 1483(w), 1441(w), 1379(m), 1325(m), 1244(s), 1130(w), 1018(m), 855(vs), 839(vs), 758(s), 677(s), 652(m), 619(w), 482(m), 461(m). IR (toluene)(cm^{-1}): 1608(vw), 1578(m,sh), 1568(m), otherwise within ±3 cm^{-1} the same as in KBr. UV–vis (λ_{max}, toluene): 970(br) < 380(sh) nm. EI-MS (direct inlet, 70 eV, 140–150 °C; m/e(%)): 516(M^+, trace). The most abundant ions are m/z 346 $[Me_2Si(C_5Me_4)_2Ti]^+$ and ions of BTMSA m/z 170, 155, 97, 73, 70 $(M - 2Me)^{2+}$. They apparently arise from the thermolysis of **3** on the surface of the ionization chamber before ionization of **3**.

2.7. Preparation of $Me_2Si(\eta^5\text{-}C_5H_4)_2Ti[\eta^2\text{-}C_2(SiMe_3)_2]$ (4)

$Me_2Si(C_5H_4)_2TiCl_2$ (**5**) (1 mmol, 0.35 g) and magnesium turnings (1 g atom, 0.0243 g) and BTMSA (0.25 ml, 1.1 mmol) in THF 20 ml) were stirred at 60 °C until all the magnesium disappeared (24 h). The brownish yellow solution was evaporated and the residue was extracted with hexane. The yellow solution was evaporated in vacuo and the yellow residue was extracted by condensing hexane vapour to separate the yellow product from a small amount of a white solid, apparently $MgCl_2$. The yield of yellow solid was 0.26 g (65%).

^{1}H NMR (C_6D_6): δ −0.330 (6 H, s, Me_2Si), −0.299 (18 H, s, Me_3Si), 5.045 (4 H, t, J = 2.4 Hz, Cp), 5.057 (4 H, t, J = 2.4 Hz, Cp). ^{13}C NMR (C_6D_6): δ −6.00 (q, 2 C), 0.59 (q, 6 C), 121.81 (d, 8 C), 126.85 (s, 2 C), 248.93 (s, 2 C). IR (hexane)(cm^{-1}): 1716(w), 1681(s), 1640(m), 1585(w), 1309(w), 1247(vs), 1237(vs), 1168(s), 1071(w), 1041(s), 900(m), 850(vs), 790(vs), 747(s), 687(m), 675(s), 646(m), 618(w), 471(s). UV–vis

Table 2
Crystallographic data and experimental details for **1–3**

	1	**2**	**3**
Crystal data			
Chem. formula	$C_{20}H_{30}Cl_2SiTi$	$C_{20}H_{30}ClSiTi$	$C_{28}H_{48}Si_3Ti$
Mol. wt. (g mol^{-1})	417.35	381.88	516.85
Crystal system	triclinic	monoclinic	triclinic
Space group	$P\bar{1}$, No.2	$P2_1/c$, No.14	$P\bar{1}$, No.2
a (Å)	8.769(3)	8.783(1)	9.403(3)
b (Å)	8.965(3)	14.861(1)	9.841(3)
c (Å)	14.452(5)	15.683(1)	17.100(4)
α (deg)	86.74(3))	90	85.52(3)
β (deg)	83.20(3)	105.530(8)	86.26(3)
γ (deg)	115.61(2)	90	71.39(2)
V (Å^3)	1010(1)	1972.3(3)	1494(1)
Z	2	4	2
D_{calc} (g cm^{-3})	1.373	1.286	1.149
μ(Mo Kα) (cm^{-1})	6.85	6.28	3.75
Approx. crystal size (mm^3)	1.0 × 0.3 × 0.1	0.2 × 0.3 × 0.5	0.5 × 0.5 × 0.2
Data collection and refinement			
$2\theta_{max}$ (deg)	50	25.48	50
Number of collected reflections	3578	3896	4358
Number of unique observed reflections, total	3350	3656	3846
$F_o > n(F_o)$	3113 (n = 2)	2808 (n = 2)	3087 (n = 2)
No. of variables	219	328	290
R	0.059	—	0.045
R_w	0.051	—	0.050
$R1$, $wR2$ (all data)	—	0.0603, 0.1075	—
$R1$, $wR2$ [$I > 2\sigma(I)$]	—	0.0374, 0.0967	—

(λ_{max}, hexane): 1050(br) nm. EI-MS (direct inlet, 75 eV, 80 °C; *m/e* (%): 404($M^{+\cdot}$; 0.5), 331([M − $SiMe_3$]$^+$; 0.1), 234([M − BTMSA]$^+$; 22.4) and the ions 170(7.5), 155(100), 73(30.1), 70(10.0) in mutual intensities corresponding to free BTMSA. The complex partly dissociates on the hot walls of the ionization chamber with elimination of BTMSA. The ionization of [$Me_2Si(\eta^5$-$C_5H_4)_2Ti$] may contribute to the intensity of *m/z* 234.

2.8. Thermolysis of 3

A saturated toluene solution of **3** (5 ml) was evaporated and the residue was dissolved in 5 ml of *m*-xylene. This solution was gradually heated to 200 °C in a sealed ampoule with only negligible darkening of the colour, and the absorption band of **3** at 970 nm decreased only slightly in intensity. Finally, heating to 210 °C for 5 h turned the colour to brown and the intensity of the absorption band diminished to ca. 15%. All volatiles were distilled into a trap cooled by liquid nitrogen and the residue was extracted by 5 ml of hexane. The brown hexane solution was silent in EPR and gave a continuous absorption decreasing in intensity from the UV to the NIR region. The residue was dissolved in toluene to give a yellow solution. This showed several EPR signals of weak intensity. Spots of green, red and yellow materials were observed after slow evaporation of toluene. None of them was isolated and identified. The volatiles contained besides *m*-xylene a mixture of *cis*- and *trans*-1,2-bis(trimethylsilyl)ethene (cf. Ref. [21]).

Table 3
Atom coordinates and equivalent isotropic temperature factors for non-hydrogen atoms in **1**

Atom	*x*	*y*	*z*	U_{eq} (Å^2)
Ti	0.1889(1)	0.2199(1)	0.2251(1)	0.029(1)
Cl(1)	0.4675(2)	0.2490(2)	0.2145(1)	0.048(1)
Cl(2)	0.2659(2)	0.5041(2)	0.1912(1)	0.052(1)
Si	−0.1871(2)	−0.0988(2)	0.2714(1)	0.036(1)
C(1)	0.1109(6)	0.0366(6)	0.3705(4)	0.035(3)
C(11)	0.1424(7)	−0.1157(6)	0.3852(4)	0.048(4)
C(2)	0.2207(6)	0.1932(6)	0.3976(4)	0.037(3)
C(21)	0.3813(7)	0.2293(7)	0.4387(4)	0.054(4)
C(3)	0.1451(6)	0.3000(6)	0.3878(4)	0.039(3)
C(31)	0.2120(7)	0.4757(6)	0.4165(4)	0.054(4)
C(4)	−0.0140(6)	0.2129(6)	0.3546(4)	0.034(3)
C(41)	−0.1389(7)	0.2865(7)	0.3471(4)	0.051(4)
C(5)	−0.0380(6)	0.0460(6)	0.3460(4)	0.033(3)
C(6)	0.1214(6)	−0.0071(6)	0.1309(4)	0.036(3)
C(61)	0.1592(7)	−0.1534(6)	0.1530(4)	0.048(4)
C(7)	0.2337(7)	0.1336(6)	0.0631(4)	0.039(3)
C(71)	0.3972(7)	0.1538(7)	0.0065(4)	0.050(4)
C(8)	0.1592(6)	0.2411(6)	0.0525(4)	0.036(3)
C(81)	0.2237(7)	0.3922(7)	−0.0177(4)	0.054(4)
C(9)	−0.0055(6)	0.1686(6)	0.1129(4)	0.034(3)
C(91)	−0.1299(7)	0.2443(7)	0.1126(4)	0.047(4)
C(10)	−0.0312(6)	0.0118(6)	0.1604(4)	0.032(3)
C(12)	−0.2427(7)	−0.3253(6)	0.2979(4)	0.052(4)
C(13)	−0.4006(6)	−0.0993(7)	0.2803(4)	0.050(4)

Table 4
Atom coordinates ($\times 10^4$) and equivalent isotropic temperature factors for non-hydrogen atoms in **2**

Atom	*x*	*y*	*z*	U_{eq} (pm^2)
Ti	2807(1)	758(1)	2562(1)	30(1)
Cl	814(1)	−268(1)	1946(1)	81(1)
Si	5575(1)	2100(1)	3376(1)	37(1)
C(1)	4240(3)	1342(2)	1610(2)	35(1)
C(11)	5722(4)	961(3)	1435(2)	50(1)
C(2)	2715(3)	1188(2)	1042(2)	41(1)
C(21)	2312(6)	578(3)	257(2)	61(1)
C(3)	1647(3)	1738(2)	1324(2)	44(1)
C(31)	−104(4)	1816(3)	877(3)	68(1)
C(4)	2474(3)	2247(2)	2067(2)	37(1)
C(41)	1705(4)	2980(2)	2464(3)	53(1)
C(5)	4126(3)	2011(2)	2251(2)	32(1)
C(6)	4983(3)	183(2)	3631(2)	33(1)
C(61)	6418(4)	−231(2)	3435(3)	49(1)
C(7)	3705(3)	−337(2)	3744(2)	36(1)
C(71)	3526(5)	−1332(2)	3664(3)	53(1)
C(8)	2654(3)	245(2)	4011(2)	37(1)
C(81)	1152(5)	−57(3)	4217(3)	58(1)
C(9)	3258(3)	1126(2)	4074(2)	36(1)
C(91)	2558(5)	1902(3)	4462(3)	55(1)
C(10)	4745(3)	1108(2)	3843(2)	34(1)
C(12)	7714(4)	1984(3)	3404(3)	58(1)
C(13)	5543(5)	3194(3)	3954(3)	63(1)

2.9. The reaction of 3 with 1-hexyne

Compound **3** (0.15 g, 0.3 mmol), toluene (5 ml) and 1-hexyne (1 ml, 9 mmol) were mixed in a bulb attached to a quartz cuvette (d = 1 mm). As indicated by the disappearance of the absorption band at 970 nm compound **3** was consumed after the reaction time of 2 weeks at room temperature. A light orange solution exerted an absorption increasing in intensity from 500 nm to shorter wavelengths. Most of the volatiles were distilled at 90 °C in vacuo into a trap cooled by liquid nitrogen and the residual orange oil (0.3 ml) was dissolved in 1 ml of hexane. The distillate contained besides toluene and less volatile products about 14% of the charged 1-hexyne. The 1-hexyne and most of the toluene were distilled off under reduced pressure. The remainder contained besides 8% of toluene the products of the 1-hexyne oligomerization consisting of the head-to-tail dimer 97%, an unidentified dimer 2% and a mixture of cyclic trimers less than 1%. The hexane solution of the oily residue was analysed by GC and by IR spectroscopy. According to GC analysis it contained a trace of the head-to-head dimer and a large amount of mainly two cyclic trimers. The only absorption band in the region 1580–2300 cm^{-1} attributable to a deactivation product of **3** was a weak narrow band at 2080 cm^{-1}. The total of converted 1-hexyne (86%) corresponded to a turnover

number of 23 mmol of 1-hexyne per 1 mmol of Ti. The correction made for the trimers contained in the orange residue gave an estimate of the product composition: head-to-tail dimer 72%, other dimer 1.5% and cyclic trimer 26%. The same procedures were recently applied for the investigation of the acetylene oligomerizations by non-bridged titanocene-BTMSA complexes [22].

2.10. X-ray crystal structure analyses of 1–3

A claret crystal fragment of **1** was stuck on a glass fibre. A brown crystal fragment of **2** and a red transparent platelet of **3** were mounted into Lindemann glass capillaries under purified nitrogen and closed with sealing wax. The X-ray measurements were carried out on a Huber four-circle diffractometer for **1**, on an Enraf–Nonius CAD-4 diffractometer for **2**, and on a Philips PW 1100 four-circle diffractometer for **3**, all at room temperature. Graphite-monochromated Mo Kα radiation ($\lambda = 0.71069$ Å) was used in all cases. The structures were solved by Patterson and Fourier methods which revealed the locations of the non-hydrogen atoms. Their coordinates and anisotropic thermal parameters were refined using SHELX-76 [1] (**1** and **3**) or SHELXL-93 [29] (**2**) programs. All hydrogen atoms were constrained to idealized geometries with fixed C–H distances. The PC ULM-package [2] [30] was used for the further calculations. Crystal data are summarized in Table 2. The atomic coordinates and thermal parameters for **1**, **2**, and **3** are given in Tables 3–5 respectively.

Table 5
Atom coordinates and equivalent isotropic temperature factors for non-hydrogen atoms in **3**

Atom	x	y	z	U_{eq} (Å^2)
Ti	0.4312(1)	0.2516(1)	0.2798(1)	0.032(1)
Si(1)	0.6874(1)	0.1019(1)	0.4023(1)	0.046(1)
Si(2)	0.1254(1)	0.5762(1)	0.1979(1)	0.054(1)
Si(3)	0.2329(2)	0.1812(2)	0.1057(1)	0.062(1)
C(1)	0.3657(4)	0.2628(4)	0.4189(2)	0.041(3)
C(11)	0.3692(5)	0.3802(5)	0.4704(3)	0.061(4)
C(2)	0.2322(4)	0.2636(4)	0.3851(2)	0.043(3)
C(21)	0.0817(4)	0.3745(5)	0.3943(3)	0.060(4)
C(3)	0.2603(4)	0.1313(4)	0.3507(2)	0.042(3)
C(31)	0.1431(5)	0.0838(5)	0.3164(3)	0.061(4)
C(4)	0.4119(4)	0.0482(4)	0.3632(2)	0.042(3)
C(41)	0.4778(5)	−0.1049(4)	0.3380(3)	0.060(4)
C(5)	0.4798(4)	0.1282(4)	0.4061(2)	0.039(3)
C(6)	0.6310(4)	0.3504(4)	0.2897(2)	0.042(3)
C(61)	0.6238(5)	0.4664(5)	0.3444(3)	0.059(4)
C(7)	0.5908(4)	0.3825(4)	0.2094(2)	0.045(3)
C(71)	0.5425(5)	0.5291(5)	0.1689(3)	0.068(4)
C(8)	0.6246(4)	0.2521(5)	0.1737(2)	0.045(3)
C(81)	0.6150(5)	0.2375(7)	0.0882(2)	0.074(5)
C(9)	0.6856(4)	0.1389(4)	0.2301(2)	0.044(3)
C(91)	0.7488(5)	−0.0167(5)	0.2085(3)	0.064(4)
C(10)	0.6909(4)	0.1981(4)	0.3033(2)	0.039(3)
C(12)	0.7569(5)	0.1795(6)	0.4823(3)	0.072(5)
C(13)	0.8064(5)	−0.0908(5)	0.4114(3)	0.070(4)
C(14)	0.2582(4)	0.3921(4)	0.2141(2)	0.040(3)
C(15)	0.2928(4)	0.2668(4)	0.1855(2)	0.039(3)
C(16)	0.1552(6)	0.6965(5)	0.2692(4)	0.086(5)
C(17)	0.1491(6)	0.6549(6)	0.0968(3)	0.084(5)
C(18)	−0.0741(5)	0.5761(6)	0.2111(4)	0.083(5)
C(19)	0.2578(7)	0.2673(8)	0.0056(3)	0.089(6)
C(20)	0.0299(7)	0.1938(9)	0.1158(3)	0.110(7)
C(22)	0.3460(8)	−0.0126(7)	0.1048(3)	0.102(6)

3. Results and discussion

3.1. Synthesis of 1–4

Compound **1** was obtained by the reaction of the lithium salt of bis(2,3,4,5-tetramethylcyclopentadienyl)dimethylsilane dianion with one equivalent of $TiCl_4$ following the method described by Jutzi and Dickbreder [26]. The low yield of 36% is probably due to a general formation of by-product polytitanium complexes bridged by the ansa-ligands and a rapid oxidation of the cyclopentadienyl anions by $TiCl_4$ yielding the ligands linked due to the recombination of the cyclopentadienyl radicals. Compound **2** was obtained in high yield by the reduction of **1** by one equivalent of BuLi. Compounds **3** and **4** were obtained in moderate yields by the general method consisting in the reduction of **1** or **5** by magnesium in the presence of BTMSA (see Scheme 1). The formation of **3** and **4** is not in contradiction with the previous observation that ansa-dimethylene-bridged titanocene monochloride $(CH_2)_2(C_5H_4)_2TiCl$ is not reduced to Ti^{II} species except in the presence of CO yielding $(CH_2)_2(C_5H_4)_2Ti(CO)_2$ [20]. The presence of BTMSA in the coordination sphere of the titanium atom facilitates the formal reduction of Ti^{III} to Ti^{II} which actually results in placing the d electrons into π^* orbitals of the acetylene [21], similar to the analogous stabilization of the titanocene dicarbonyls.

3.2. Crystal structures of 1–3

Compounds **1–3** have the usual bent sandwich structures common to non-bridged titanocene derivatives, e.g. $(C_5H_5)_2TiCl_2$ [31], $(C_5H_4Me)_2TiCl_2$ [32], $(C_5HMe_4)_2TiCl_2$ [33], $(C_5Me_5)_2TiCl_2$ [34], $(C_5HMe_4)_2TiCl$ [33], $(C_5Me_5)_2TiCl$ [35], $(C_5HMe_4)_2Ti \cdot BTMSA$ [21], and $(C_5Me_5)_2Ti \cdot BTMSA$ [36]. Compound **1** is also comparable with its non-methylated congener, $Me_2Si(\eta^5\text{-}C_5H_4)_2TiCl_2$ (**5**) [15] and the dimethylmethylene analogue $Me_2C(\eta^5\text{-}C_5H_4)_2TiCl_2$ (**6**)

[1] See footnote 2.

[2] The ULM-Programmsystem includes SHELX-76 (G.M. Sheldrick, *Program for Crystal Structure Determination*, University of Cambridge, Cambridge, UK, 1976).

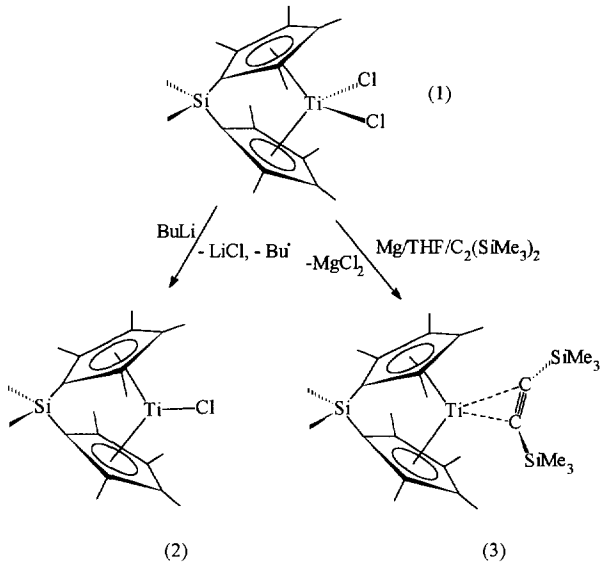

Scheme 1.

[37]. Isolated molecules **1–3** possess *mm*2 symmetry. Nevertheless, in the crystals all atoms are placed in general positions. In contrast, molecules **5** and **6**, also having *mm*2 symmetry, sit on crystallographic symmetry elements 2 and *m* respectively. The molecular structures of **1**, **2**, and **3** with atom numbering schemes are shown in Figs. 1–3, and selected bond distances and bond angles are gathered in Table 6. The geometry of the titanocene skeletons in **1–3** and in similar relevant complexes is described by the parameters listed in Table 7. They comprise the Ti–CE (CE is the centroid of the cyclopentadienyl ring) distance, the CE–Ti–CE angle, the distance D of the Ti atom from the interconnection of CE(1) and CE(2) [37], its difference Δ from that for a standard complex, the angle ϕ between the least-squares planes of the cyclopentadienyl rings, the cyclopentadienyl ring slippage angle α (the angle between the Ti–CE interconnection and the ring plane towards the bridge), and the angle β between the ring plane and the bond from the ring atom to the bridging element

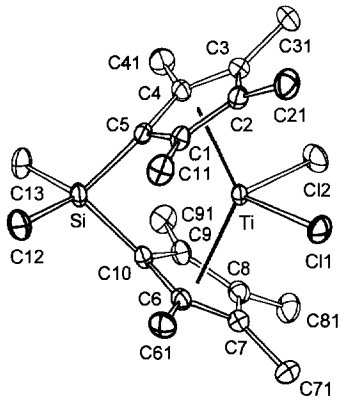

Fig. 1. ORTEP diagram of **1** with 30% probability thermal ellipsoids and the atom numbering scheme.

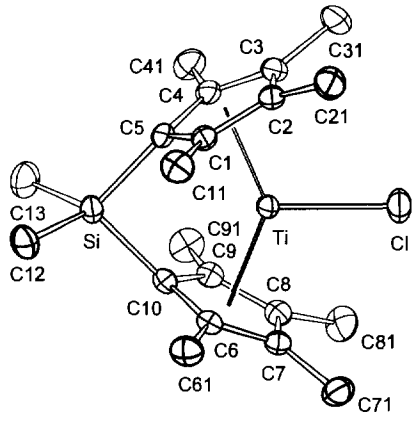

Fig. 2. ORTEP diagram of **2** with 30% probability thermal ellipsoids and the atom numbering scheme.

(Si,C) (see Fig. 4). The distance D and $\Delta(\%)$ visualize the difference in the CE–Ti–CE angle corrected for the particular Ti–CE distance; at variance with the originally used $(C_5H_5)_2TiCl_2$ standard [37], which is, however, poorly defined by two different and non-symmetrical molecules in the unit cell [31], the data for $(C_5H_4Me)_2TiCl_2$ which has a crystallographic mirror plane containing Ti and both Cl atoms [32], were taken as a standard. The size of the coordination space at the open side of the titanocene moieties is determined mainly by the magnitude of angle ϕ; the larger is ϕ, the larger is the coordination space. This space is further diminished by the decrease in the Ti–CE and D distances. The angle β indicates the distortion from the sp^2 hybridization at the cyclopentadienyl ring carbon atom connected to the bridge element.

The largest difference in the structures **1–3** follows from the different types of coordination. The coordination is pseudotetrahedral in **1** and **3** whereas it is pseudotrigonal in **2**. As a result, the Ti–CE distance in **2** is by 0.1 Å shorter than that in **1** and about 0.06 Å shorter than that in **3**. The Ti–Cl bond length in **2** is, however, only negligibly shorter than that in **1**. Another consequence of the pseudotrigonal coordination is a much larger CE–Ti–CE angle in **2** than in the other two compounds. On the other hand, the large difference

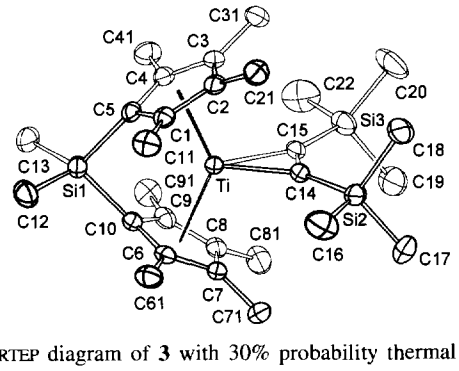

Fig. 3. ORTEP diagram of **3** with 30% probability thermal ellipsoids and the atom numbering scheme.

Table 6
Selected bond distances (Å) and bond angles (deg) for **1–3**

	1	2	3
Distances			
Ti–CE(1)	2.140(5)	2.046(3)	2.120(4)
Ti–CE(2)	2.132(5)	2.047(3)	2.110(4)
Ti–C(1)	2.426(6)	2.361(3)	2.419(4)
Ti–C(2)	2.552(6)	2.448(3)	2.491(4)
Ti–C(3)	2.532(6)	2.423(3)	2.487(4)
Ti–C(4)	2.403(5)	2.338(3)	2.413(4)
Ti–C(5)	2.373(5)	2.313(2)	2.389(4)
Ti–C(6)	2.410(6)	2.341(3)	2.395(4)
Ti–C(7)	2.546(6)	2.433(3)	2.473(4)
Ti–C(8)	2.543(6)	2.434(3)	2.485(4)
Ti–C(9)	2.409(5)	2.362(3)	2.422(4)
Ti–C(10)	2.365(5)	2.318(3)	2.383(4)
Si(1)–C(5)	1.893(5)	1.883(3)	1.883(4)
Si(1)–C(10)	1.885(5)	1.879(3)	1.879(4)
Si(1)–C(12)	1.876(6)	1.875(4)	1.864(5)
Si(1)–C(13)	1.859(6)	1.865(4)	1.870(5)
Ti–Cl(1)	2.327(2)	2.327(1)	—
Ti–Cl(2)	2.340(2)	—	—
Ti–C(14)	—	—	2.093(4)
Ti–C(15)	—	—	2.105(4)
C(14)–C(15)	—	—	1.297(5)
Si(2)–C(14)	—	—	1.855(4)
Si(2)–C(Me)$_{av}$	—	—	1.866(6)
Si(3)–C(15)	—	—	1.863(4)
Si(3)–C(Me)$_{av}$	—	—	1.873(6)
Angles			
CE(1)–Ti–CE(2)	132.2(2)	137.0(1)	133.1(1)
C(5)–Si–C(10)	91.8(2)	94.3(1)	95.3(2)
C(12)–Si–C(13)	102.9(3)	102.3(2)	101.8(2)
Cl–Ti–Cl(2)	95.9(1)	—	36.0(1) [a]
ϕ [b]	59.3	51.1	53.5

[a] The value of the C(14)–Ti–C(15) angle.
[b] The angle between the least-squares planes of the cyclopentadienyl rings.

between the Cl(1)–Ti–Cl(2) angle of 95.9(1)° in **1** and the C(14)–Ti–C(15) angle of 36.0(1)° in **3** influences the CE–Ti–CE angle only by ca. 1° in the expected direction. Inspection of the data in Table 7 reveals that the dimethylsilylene bridge diminishes the differences in the CE–Ti–CE angle between the dichlorides, monochlorides and BTMSA complexes only by about 1° compared to the same series of complexes with the $(C_5HMe_4)_2Ti$ and $(C_5Me_5)_2Ti$ moieties. The data also show that the most oblique slippage angles α within each of the three series of compounds are obtained for **1–3**. On the other hand, the C_5Me_5 compounds have the angle α very close to 90° in spite of the steric hindrance between the Me groups near the 'hinge' position of the permethylated ligands. The steric hindrance is, however, reflected in the maximum values of the CE–Ti–CE angles and the minimum values of ϕ. The values of the CE–Ti–CE, ϕ, and α angles of the C_5HMe_4 compounds fall between those of the ansa-$Me_2Si(C_5Me_4)$ and the C_5Me_5 compounds.

The comparison of the monosubstituted ring structures in $(C_5H_4Me)_2TiCl_2$, **5**, and **6** shows that the value of the CE–Ti–CE angle strongly decreases in the order $(C_5H_4Me)_2TiCl_2 > 5 \gg 6$ whereas that of ϕ decreases in the order $6 > (C_5H_4Me)_2TiCl_2 > 5$. Compound **6** shows the smallest value of the CE–Ti–CE angle and, correspondingly, the largest distance D; surprisingly, the ring slippage angle α is oblique (85.8°) (cf. [37]). The data for **5** demonstrate that the Me_2Si bridge imposes only a slight change compared to the skeleton angles in non-bridged $(C_5H_5)_2TiCl_2$ [31] and $(C_5H_4Me)_2TiCl_2$ [32] although the value of β (19.1°) implies a considerable strain, higher than in **1** and comparable with the strain in **2** and **3**. There is no apparent objection for compound **5** to release this strain by enlarging ϕ and decreasing α, in the way that occurs in **1** or **6**. The large value of β in **5** can hardly be brought about by an intramolecular attractive interaction of ring hydrogen atoms with the chlorine ligands [38] since a similar result of such an effect is not observed in **6**. Hence, it has to be assumed that the geometry of bent sandwich compounds is non-negligibly controlled by intermolecular interactions [38] and/or by crystal packing effects (see also Ref. [39]).

3.3. Properties of 2

The EPR investigation of **2** in toluene and MTHF solutions and frozen glasses proved that the compound was monomeric. The results of these studies are gathered in Table 1. In toluene, a broad single line (ΔH = 10 G) at $g = 1.9725$ was observed at room temperature, and this turned into a strongly anisotropic spectrum upon cooling to −130 °C. The low-field g-tensor components g_z and g_x have the values typical of $(C_5H_{5-n}Me_n)_2Ti^{III}$ species [28] and g_y falls into the range corresponding to a trigonal coordination of the Ti atom as is known from the monomeric $(C_5H_{5-n}Me_n)_2TiX$ (n = 3–5, X = Cl, Br and I) complexes [1]. No evidence was detected for the dimerization of **2** that would give a triplet state dimer [40]. In MTHF solution, in addition to a broad line of **2** at $g = 1.9726$, virtually identical with that observed in

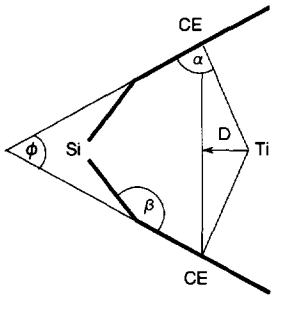

Fig. 4. Scheme of angles and distances in the symmetrical ansa-titanocene skeleton.

Table 7
Important lengths (Å) and angles (deg) in **1**–**3** and some related complexes

	CE–Ti–CE (deg)	Ti–CE (Å)	D (Å) [a]	Δ (Å) [b]	Δ (%) [b]	ϕ (deg) [c]	α (deg) [d]	β(deg) [e]	Ref.
$(C_5H_4Me)_2TiCl_2$	130.2	2.067	0.870	0	0	53.3	88.25	—	[32]
$(C_5HMe_4)_2TiCl_2$	133.4	2.109	0.835	−0.035	−4	54.4 *	86.1	—	[33]
$(C_5Me_5)_2TiCl_2$	137.4	2.127	0.773	−0.097	−11	44.6 *	89.0	—	[34]
1 $Me_2Si(C_5Me_4)_2TiCl_2$	132.2	2.136	0.865	−0.005	−1	59.3	84.2	16.2	This work
5 $Me_2Si(C_5H_4)_2TiCl_2$	128.7	2.075	0.898	0.028	3	51.2	90.0	19.1	[15]
6 $Me_2C(C_5H_4)_2TiCl_2$	121.5	2.056	1.005	0.135	16	66.9 *	85.8	14.9	[37]
$(C_5HMe_4)_2TiCl$	139.1	2.031	0.710	−0.160	−18	45.5 *	87.7	—	[33]
$(C_5Me_5)_2TiCl$	143.6	2.06	0.643	−0.227	−26	36.4	90.0	—	[35]
2 $Me_2Si(C_5Me_4)_2TiCl$	137.0	2.046	0.750	−0.120	−14	51.1	85.9	21.6	This work
8 $(C_5HMe_4)_2Ti \cdot BTMSA$	134.9	2.092	0.802	−0.068	−8	50.0	87.5	—	[21]
9 $(C_5Me_5)_2Ti \cdot BTMSA$	138.6	2.114	0.747	−0.123	−14	41.1	90.1	—	[36]
3 $Me_2Si(C_5Me_4)_2Ti \cdot BTMSA$	133.1	2.115	0.842	−0.028	−3	53.5	86.7	20.9	This work

[a] D is the distance of the titanium atom from the CE(1)–CE(2) interconnection (taken from Ref. [37] or calculated as $\cos[(CE–Ti–CE)/2]d(Ti–CE)$.
[b] Δ is the difference of D from the value for $(C_5H_4Me)_2TiCl_2$.
[c] ϕ is the angle between the least-squares planes of the cyclopentadienyl rings (the data with asterisk were calculated from coordinates using the PC-ULM package [30]).
[d] α is the angle between the least-squares plane of the cyclopentadienyl ring and the Ti–CE interconnection.
[e] β is the angle between the least-squares plane of the cyclopentadienyl ring and the bond of the ring atom to the bridging element M(Si,C) (calculated as $[(C_{Cp}–M–C_{Cp}) - \phi]/2$).

toluene, a weak and sharp single line occurred at $g = 1.9826$ displaying low-intensity wing multiplets due to the coupling to ^{47}Ti and ^{49}Ti isotopes ($a_{Ti} = 10$ G). This signal grew in intensity with decreasing temperature on account of the signal intensity of **2**. In frozen MTHF glass at −140 °C a nearly symmetrical g-tensor indicated a pseudotetrahedral environment of the Ti^{III} ion in the complex of **2** with MTHF (denoted **2a**). This behaviour of **2** towards MTHF proves its ability to coordinate one molecule of MTHF and shows that the equilibrium in Eq. (1) is shifted to the product side with lowering of the temperature.

$$Me_2Si(C_5Me_4)_2TiCl + MTHF \Leftrightarrow Me_2Si(C_5Me_4)_2TiCl(MTHF)\ (\mathbf{2a}) \quad (1)$$

In the series of the $(C_5H_{5-n}Me_n)_2TiCl$ compounds the ability to coordinate MTHF decreases with increasing number of Me groups on the cyclopentadienyl rings. Whereas the chlorides for $n = 0$, 1 and 2 coordinate MTHF at room temperature [41], $(C_5HMe_4)_2TiCl$ does not coordinate MTHF at ambient temperature and $(C_5Me_5)_2TiCl$ remains uncoordinated even at 77 K [1]. The above-described temperature-dependent behaviour of **2** towards MTHF closely resembles the behaviour of $(C_5H_2Me_3)_2TiCl$ [1], and this implies that the bridging Me_2Si group exerts an electron withdrawing effect compensating the electron donation effect of two Me groups. The EPR parameters g_{iso}, g_{av}, and g_y of **2** and **2a** fall outside the range of values of the $(C_5H_{5-n}Me_n)_2TiCl$ compounds [1] and cannot be used for the estimation of the electronic effect of the μ-$SiMe_2$ group. The reason can be sought in a through space interaction of the titanium d_{xz} and d_{z^2} orbitals with the silicon orbital of suitable symmetry (see the suggested model in Ref. [28]) which may change the energies of $1a_1$ and b_2 MO levels.

The difference in the electronic structure of brown compound **2** with respect to blue $(C_5H_{5-n}Me_n)_2TiCl$ ($n = 3$–5) compounds is also reflected in the UV–vis spectra. The long-wavelength band of **2** has the maximum at 525 nm and a shoulder at 600 nm whereas the above titanocene compounds have the maxima at 540–560 nm and the shoulder at 620–640 nm. The short-wavelength region with the intense band at 350 nm and two well-discernible shoulders at 410 and 450 nm is also at variance with the spectra of the above titanocene compounds which display a poorly resolved shoulder in the region 340–360 nm only. The assignment of the electronic bands of **2** is beyond the scope of this work.

3.4. Properties of 3 and 4

The IR, ^1H and ^{13}C NMR and UV–vis spectra of **3** and **4** bear all the features typical of the non-ansa titanocene–BTMSA complexes $(C_5H_{5-n}Me_n)_2Ti[\eta^2$-$C_2(SiMe_3)_2]$ ($n = 0$–5) [21] (see Table 8). The strength of the coordination bond between the Ti atom and BTMSA is usually estimated from the valence vibration ν(C≡C) of the coordinated triple bond and from ^{13}C NMR chemical shift δ(C≡C) [21,36]. The shift of ν(C≡C) to lower wavenumbers reliably reflects the strength of acetylene coordination since the UV–vis spectra prove that the electronic structure of all the compared compounds is essentially the same (vide infra). In spite of some uncertainty resulting from the occurrence of several absorption bands in the relevant

Table 8
NMR, IR and NIR data on the BTMSA ligand in **3**, **4**, $(C_5H_5)_2Ti[\eta^2\text{-}C_2(SiMe_3)_2]$ (**7**), $(C_5HMe_4)_2Ti[\eta^2\text{-}C_2(SiMe_3)_2]$ (**8**), and $(C_5Me_5)_2Ti[\eta^2\text{-}C_2(SiMe_3)_2]$ (**9**)

Compound	^{1}H(Me) (δ ppm)	^{13}C(Me) (δ ppm)	^{13}C(C≡C) (δ ppm)	ν(C≡C) (cm^{-1})	λ (nm)	Ref.
3	−0.054	4.20	254.86	1585	970	This work
4	−0.299	0.59	248.93	1655	1050	This work
7	−0.333 s	0.59 q	244.77	1662	1060	[21]
8	−0.049 s	3.46 q	248.35	1609	920	[21]
9	0.016 s	4.23 q	248.51 s	1598	916	[21]

region [21], the average ν(C≡C) values obtained in solution (see Table 8) indicate that the Ti–BTMSA bond in **4** is somewhat stronger than in $(C_5H_5)_2Ti[\eta^2\text{-}C_2(SiMe_3)_2]$ (**7**) and much weaker than in $(C_5HMe_4)_2Ti[\eta^2\text{-}C_2(SiMe_3)_2]$ (**8**) and $(C_5Me_5)_2Ti[\eta^2\text{-}C_2(SiMe_3)_2]$ (**9**). The lowest value of ν(C≡C) was observed in **3**. Hence, the strength of the Ti–BTMSA bond increases in the order: **7** < **4** < **8** < **9** < **3**.

The data of δ(C≡C) in Table 8 give the order of down-field shifts **7** < **8** < **9** < **4** < **3**. This differs from the order of ν(C≡C) values, and the values of δ(C≡C) for the ansa- and non-ansa-compounds are not compatible. The difference of δ(C≡C) between **3** and **9** is larger than between **7** and **9** and the non-methylated ansa-compound **4** has its δ(C≡C) value down-field shifted with respect to the permethylated compound **9**. These comparisons show that the down-field shift of δ(C≡C) can be used to estimate the strength of the acetylene coordination only within the same structural type, i.e. titanocenes or ansa-titanocenes.

Another important feature of the titanocene–BTMSA complexes is a long-wavelength electronic absorption band occurring in the NIR region (Table 8). The positions of the band do not give any correlation for the set of compounds listed in Table 8, except that λ_{max} decreases with the increasing strength of the BTMSA coordination in both the ansa- (**3**,**4**) and non-ansa- (**7**–**9**) series of compounds. This band is probably of d → π^* type [21] since the bonding between Ti(II) and BTMSA can be imagined as involving a strong interaction of filled π-orbitals of acetylene with the $2a_1$ Ti orbital and the back-bonding interaction of the Ti(II) b_2 orbital with the empty π^* orbital [42].

The thermal stability of **3** is of interest because large differences in the behaviour of $(C_5HMe_4)_2Ti$(BTMSA) (**8**) and $(C_5Me_5)_2Ti$(BTMSA) (**9**) have recently been observed [21,22]. Heating of **3** in *m*-xylene to 200 °C did not lead, as judged from the persistence of the absorption band of **3** at 970 nm, to the observable thermolysis. The band intensity decreased to ca. 15% of the initial value only after heating to 210 °C for 5 h. The thermolysis afforded a mixture of products which all were similarly soluble in toluene. Their low solubility in hexane indicates that compound **3** does not yield monomeric μ-$SiMe_2(\eta^5\text{-}C_5Me_4)(\eta^3{:}\eta^4\text{-}$2,5-dimethyl-3,4-dimethylenecyclopentenyl)Ti(II), an analogue of the allyl-diene [43] products which arise from the thermolysis of **8** and **9** [21], although the hydrogen transfer from probably an ansa-titanocene moiety to BTMSA occurred, yielding cis- and trans-isomers of $(Me_3Si)HC{=}CH(SiMe_3)$. A low yield and a number of products of similar solubility precluded the isolation and identification of some of the components.

The catalytic activity of **3** towards 1-hexyne has been of interest because the linear head-to-tail dimerization of 1-alkynes is believed to be controlled by the steric congestion in the highly methyl-substituted titanocene skeleton [44]. A sharp difference in the activity and selectivity of complexes **8** and **9** has been recently correlated with the value of angle ϕ in the solid state structures. Complex **9** (1 mmol) converts 1.2–1.5 mol of 1-hexyne to 2-butyl-1-octen-3-yne with the selectivity better than 98%, and the next member, complex **8**, attains the turnover of only 7 mmol of 1-hexyne per 1 mmol of Ti and produces 21% of 2-butyl-1-octen-3-yne in addition to cyclotrimers [22]. Compound **3** (1 mmol) converts 23 mmol of 1-hexyne into oligomers containing 72% of 2-butyl-1-octen-3-yne, and this places the catalytic activity and selectivity of **3** to be intermediate between those of **8** and **9**. Whereas the superior turnover number and the selectivity of **9** are compatible with the smallest size of the coordination space yielded by the $(C_5Me_5)_2Ti$ skeleton, a considerably better selectivity of **3** compared to that of **8** would imply a smaller coordination space and hence, smaller values of ϕ and D for **3** than for **8**. This is, however, in contradiction with the crystallographic molecular parameters (see Table 7). We suggest that the inconsistency of the crystallographic and catalytic parameters of **3** and **8** may be brought about by a larger flexibility of the titanocene skeleton in **8** affording a larger effective coordination space in the critical moment of coordination of the further acetylene molecule(s) than the more rigid skeleton of **3**.

3.5. Conclusions

The molecular structures of titanocene and ansa-titanocene dichlorides, monochlorides and bis(trimethyl-

silyl)acetylene complexes in the solid state showed that the free coordination space at the open side of the titanocene skeleton increases in the order $(C_5Me_5)_2Ti < (C_5HMe_4)_2Ti < Me_2Si(C_5Me_4)_2Ti$. The activity and selectivity in the catalytic head-to-tail dimerization of 1-hexyne, which is believed to be sterically controlled [22,44], increases in the order **8** < **3** < **9**. A higher selectivity of **3** compared to that of **8** is accounted for by a more rigid ansa-titanocene skeleton in **3**, affording a smaller coordination space than the flexible skeleton of **8**. The affinity to MTHF indicates that the Lewis acidity of **2** is comparable to that of $(C_5H_2Me_3)_2TiCl$. The positions of the ν(C≡C) vibration in the BTMSA complexes establish the order of the increasing strength of the Ti–BTMSA bond to be **7** < **4** < **8** < **9** < **3**. The inconsistencies in the EPR g-tensor parameters of **2** and NMR ^{13}C δ(C≡C) of **3** and **4** in relation to analogous titanocene compounds show that the ansa-μ-$SiMe_2$ group influences the electron density at the Ti atom only by changing the overall basicity of the cyclopentadienyl ligands. Considering this mechanism, the values of δ(C≡C) would imply that the effect of the μ-$SiMe_2$ group (in **4**) is larger than the electron donation effect of ten Me substituents (in **9**), and this is unrealistic. Thus, the δ(C≡C) values can be used for sorting compounds within the same structural type, whereas another mechanism, probably a through-space Si–Ti interaction (cf. [28]), is to be sought to explain the effect of the μ-$SiMe_2$ group.

4. Supplementary material available

Further details of the X-ray crystal structure determinations have been deposited at the Fachinformationszentrum Karlsruhe, Gesellschaft für wissenschaftlich-technische Information mbH, D-76344 Eggenstein-Leopoldshafen and are available on quoting the deposition numbers CSD-391028 (compound **1**), CSD-391030 (compound **2**), and CSD-301029 (compound **3**). Additional information such as least-squares planes, dihedral angles and views of the unit cells may be obtained from the authors.

Acknowledgements

This investigation was supported by the Grant Agency of Academy of Sciences of the Czech Republic (Grant No. A440403) and by the Volkswagen-Stiftung. Chemetall, GmbH, Frankfurt, Germany, is acknowledged for donation of organolithium reagents. The Grant Agency of the Czech Republic (grant No. 203/96/0111) sponsored an access to the Cambridge Structure Data Base.

References

[1] K. Mach and J.B. Raynor, *J. Chem. Soc. Dalton Trans.*, (1992) 683.
[2] J. Hiller, U. Thewalt, M. Polášek, L. Petrusová, V. Varga, P. Sedmera and K. Mach, *Organometallics, 15* (1996) 3752.
[3] T. Vondrák, K. Mach and V. Varga, *Organometallics, 11* (1992) 2030.
[4] P.G. Gassman, W.H. Campbell and D.W. Macomber, *Organometallics, 3* (1984) 385.
[5] K. Mach and V. Varga, *J. Organomet. Chem., 347* (1988) 85.
[6] P.G. Gassman, D.W. Macomber and J.W. Hershberger, *Organometallics, 2* (1983) 1470.
[7] K. Mach, V. Varga, H. Antropiusová and J. Poláček, *J. Organomet. Chem., 333* (1987) 205.
[8] M.F. Lappert, C.J. Pickett, P.I. Riley and P.I.W. Yarrow, *J. Chem. Soc. Dalton Trans.*, (1981) 805.
[9] J. Okuda, *Topics Curr. Chem., 160* (1991) 99.
[10] P.G. Gassman, P.A. Deck, C.H. Winter, D.A. Dobbs and D.H. Cao, *Organometallics, 11* (1992) 959.
[11] W.C. Finch, E.V. Anslyn and R.H. Grubbs, *J. Am. Chem. Soc., 110* (1988) 2406.
[12] M. Horáček, R. Gyepes, I. Císařová, M. Polášek, V. Varga and K. Mach, *Collect. Czech. Chem. Commun., 61* (1996) 1307.
[13] H.-H. Brintzinger, D. Fischer, R. Mülhaupt, B. Rieger and R.M. Waymouth, *Angew. Chem. Int. Ed. Engl., 34* (1995) 1143 and references cited therein.
[14] S. Mansel, U. Rief, M.-H. Prosenc, R. Kirsten and H.-H. Brintzinger, *J. Organomet. Chem., 512* (1996) 225 and references cited therein.
[15] C.S. Bajgur, W.R. Tikkanen and J.L. Petersen, *Inorg. Chem., 24* (1985) 2539.
[16] J.K. Pudelski, D.A. Foucher, C.H. Honeyman, A.J. Lough, I. Manners, S. Barlow and D. O'Hare, *Organometallics, 14* (1995) 2470.
[17] R. Gómez, T. Cuenca, P. Royo, M.A. Pellinghelli and A. Tiripicchio, *Organometallics, 19* (1991) 1505.
[18] P. Royo, *New J. Chem., 14* (1990) 553.
[19] T. Cuenca, R. Gómez, P. Gómez-Sal and P. Royo, *J. Organomet. Chem., 454* (1993) 105.
[20] J.A. Smith and H.H. Brintzinger, *J. Organomet. Chem., 218* (1981) 159.
[21] V. Varga, K. Mach, M. Polášek, P. Sedmera, J. Hiller, U. Thewalt and S.I. Troyanov, *J. Organomet. Chem., 506* (1995) 241.
[22] V. Varga, L. Petrusová, J. Čejka, V. Hanuš and K. Mach, *J. Organomet. Chem., 509* (1996) 235.
[23] H. Antropiusová, A. Dosedlová, V. Hanuš and K. Mach, *Transition Met. Chem., 6* (1981) 90.
[24] V.A. Mironov, T.M. Fadeeva, E.V. Sobolev and A.N. Elizarova, *Zh. Obshch. Khim., 33* (1963) 84.
[25] J. Müller, F. Lüdemann and H. Köpf, *J. Organomet. Chem., 303* (1986) 167.
[26] P. Jutzi and R. Dickbreder, *Chem. Ber., 119* (1986) 1750.
[27] C.M. Fendrick, L.D. Schertz, V.W. Day and T.J. Marks, *Organometallics, 7* (1988) 1828.
[28] W.W. Lukens, Jr., M.R. Smith, III and R.A. Andersen, *J. Am. Chem. Soc., 118* (1996) 1719.
[29] G.M. Sheldrick, SHELXL-93, *Program for Crystal Structure Refinement*, University of Göttingen, Germany, 1993.
[30] R. Brüggemann, T. Debaerdemaeker, B. Müller, G. Schmid and U. Thewalt, ULM-Programmsystem, *1. Jahrestagung der Deutschen Gesellschaft für Kristallografie, Mainz, June 9–12, 1992*, Abstr., p. 33.
[31] A. Clearfield, D.K. Warner, C.H. Saldarriaga-Molina and R. Ropal, *Can. J. Chem., 53* (1975) 1622.

[32] J.L. Petersen and L.F. Dahl, *J. Am. Chem. Soc., 97* (1975) 6422.
[33] S.I. Troyanov, V.B. Rybakov, U. Thewalt, V. Varga and K. Mach, *J. Organomet. Chem., 447* (1993) 221.
[34] T.C. McKenzie, R.D. Sanner and J.E. Bercaw, *J. Organomet. Chem., 102* (1975) 457.
[35] J.W. Pattiasina, H.J. Heeres, F. van Bolhuis, A. Meetsma, J.H. Teuben and A.L. Spek, *Organometallics, 6* (1987) 1004.
[36] V.V. Burlakov, A.V. Polyakov, A.I. Yanovsky, Yu.T. Struchkov, V.B. Shur, M.E. Vol'pin, U. Rosenthal and H. Görls, *J. Organomet. Chem., 476* (1994) 197.
[37] R.M. Shaltout, J.Y. Corey and N.P. Rath, *J. Organomet. Chem. , 503* (1995) 205.
[38] M.E. Huttenloch, J. Diebold, U. Rief, H.H. Brintzinger, A.M. Gilbert and T.J. Katz, *Organometallics, 11* (1992) 3600.
[39] P.C. Möhring, N. Vlachakis, N.E. Grimmer and N.J. Coville, *J. Organomet. Chem., 483* (1994) 159.
[40] E. Samuel, J.F. Harrod, D. Gourier, Y. Dromzee, F. Robert and Y. Jeannin, *Inorg. Chem., 31* (1992) 3252.
[41] K. Mach, G. Schmid, V. Varga and U. Thewalt, *Collect. Czech. Chem. Commun., 61* (1996) 1285.
[42] J.W. Lauher and R. Hoffmann, *J. Am. Chem. Soc., 98* (1976) 1729.
[43] J.W. Pattiasina, C.E. Hissink, J.L. de Boer, A. Meetsma, J.H. Teuben and A.L. Spek, *J. Am. Chem. Soc., 107* (1985) 7758.
[44] H. Akita, H. Yasuda and A. Nakamura, *Bull. Chem. Soc. Jpn., 57* (1984) 480.